Atmospheric Environment 42 (2008) 7795–7811

Contents lists available at ScienceDirect

Atmospheric Environment

journal homepage: www.elsevier.com/locate/atmosenv

Application of high resolution land use and land cover data for atmospheric modeling in the Houston–Galveston metropolitan area, Part I: Meteorological simulation results

Fang-Yi Cheng, Daewon W. Byun*

Institute for Multi-dimensional Air Quality Studies, University of Houston, Houston, TX 77204-5007, USA

ARTICLE INFO

Article history:
Received 4 September 2007
Received in revised form 15 April 2008
Accepted 16 April 2008

Keywords:
Satellite-derived land use land cover data
Land surface model
MM5
Land–sea breeze

ABSTRACT

To predict atmospheric conditions in an urban environment, the land surface processes must be accurately described through the use of detailed land use (LU) and land cover (LC) data. Use of the U.S. Geological Survey (USGS) 25-category data, currently in the Fifth-generation Mesoscale Model (MM5), with the Noah land surface model (LSM) and MRF (medium-range forecast) planetary boundary layer (PBL) schemes resulted in the over-prediction of daytime temperatures in the Houston downtown area due to the inaccurate representation as a completely impervious surface. This bias could be corrected with the addition of canopy water in the urban areas from the evapotranspiration effects of urban vegetation. A more fundamental approach would be to utilize an LULC dataset that represents land surface features accurately. The Texas Forest Service (TFS) LULC dataset established with the LANDSAT satellite imagery correctly represents the Houston–Galveston–Brazoria (HGB) area as mixtures of urban, residential, grass, and forest LULC types. This paper describes how the Noah LSM and PBL schemes in the MM5 were modified to accommodate the TFS-LULC data. Comparisons with various meteorological measurements show that the MM5 simulation made with the high resolution LULC data improves the boundary layer mixing conditions and local wind patterns in the Houston Ship Channel, which is a critically important anthropogenic emission area affecting the HGB air pollution problems. In particular, when the synoptic flows are weak, the improved LULC data simulates the asymmetrically elongated Houston heat island convergence zone influencing the location of the afternoon Gulf of Mexico sea-breeze front and the Galveston Bay breeze flows.

This paper is part I of a two-part study and focuses on the meteorological simulation. In part II, effects of using the different meteorological inputs on air quality simulations are discussed.

1. Introduction

Reflecting its evolution as a mega city in the past few decades, land use (LU) and land cover (LC) characteristics in Houston have changed due to removal of vegetation and trees in the outskirts and further urbanization of different parts of the metropolitan area. Such changes may have modified the local weather conditions, including the urban heat island (UHI) effects.

To simulate atmospheric dynamic and thermodynamic processes adequately, a meteorological model requires an LULC dataset that accurately represents current environmental conditions. Several research results demonstrate that the LULC data significantly affects meteorological simulations (e.g. Lam et al., 2006; Lo and Quattrochi, 2003;

* Corresponding author. Science and Research 1 Building, Room 312, University of Houston, 4800 Calhoun Road, Houston, TX 77204-5007, USA. Tel.: +1 713 743 0707; fax: +1 713 748 7906.
E-mail address: daewon.byun@mail.uh.edu (D.W. Byun).

1352-2310/$ – see front matter © 2008 Elsevier Ltd. All rights reserved.
doi:10.1016/j.atmosenv.2008.04.055

Civerolo et al., 2005). Currently, the U.S. Geological Survey (USGS) 25-category LULC data (hereafter, USGS-LULC) available with the MM5 meteorological modeling system is roughly at 1-km resolution with the reference year 1990, and some of the components originated from a dataset compiled in the 1970s. In particular, the LULC dataset represents the center of Houston as a contiguous urban impervious surface type without resolving the detailed variations that are essential in simulating local meteorological conditions. In reality, Houston is covered with substantial amounts of trees, grasslands, and residential suburbs in addition to the urban built-up structures. Due to this coarse representation of the land use distribution in the USGS-LULC dataset, MM5 over-predicts daytime maximum temperatures as compared to real observations in the Houston downtown area (Cheng et al., 2004).

Recently, the Texas Forest Service (TFS) hired Global Environmental Management (GEM) to generate updated and more accurate LU and LC datasets separately for Houston and the surrounding eight county areas using the 30-m resolution LANDSAT satellite imagery and ancillary datasets for the reference year 2000 (GEM, 2003). The detailed description of the LULC datasets is provided in Section 2.

The primary goal of the present research is to understand the effects of using different LULC datasets in MM5 on the simulated meteorological conditions that are essential inputs for air quality simulations, such as changes in winds, surface temperature, turbulent flux fields and planetary boundary layer (PBL) structures. The secondary goal is to evaluate the performance of the MM5 simulations with the surface and wind profiler measurements obtained during the Texas Air Quality Study (TexAQS) 2000 period. Standard statistical methods were applied to evaluate the model performance in simulating the measured surface parameters.

This paper, which focuses on the meteorological simulation, is part I of a two-part study. We compare the two LULC datasets in Section 2, describe the necessary modifications of MM5 to utilize the different LULC data in Section 3, discuss the difficulties of the meteorological simulations in Section 4, and evaluate the benefits of using the high resolution LULC data in Section 5. In part II, effects of using these meteorological data from different LULC data on air quality simulations are discussed (Cheng et al., 2008).

2. Description of the land use data

The TFS has generated accurate LU and LC datasets separately for Houston and the surrounding eight county areas using the 30-m resolution LANDSAT satellite imagery taken in late September 2000 and ancillary datasets for the reference year 2000 (GEM, 2003). The updated LULC dataset covers the eight counties of Brazoria, Chambers, Fort Bend, Galveston, Harris, Liberty, Montgomery, and Waller (Fig. 1a). A supervised classification method that relies on the priori information of the spectral features of the targets was employed using image-processing software to define the LU classes (forest, range, agriculture, urban/developed) and LC classes (forest composition (coniferous, broadleaf, mixed), grass, wetland, water, barren (beach, bare soil), impervious (roads, parking lots, buildings)) (GEM, 2003). The procedure involves several steps including: (1) pre-processing the satellite data collected at different times, (2) selecting the training areas of the desired class, (3) identifying the datasets corresponding to various spectral signatures, (4) running the classification, and (5) evaluating the results (GEM, 2003). The dataset is referred to as TFS-LULC. After reviewing the TFS-LULC data, we found that a large area in Fort Bend County was classified as the barren class. For the modeling episode, from August 22 to September 1, 2000, the actual land cover was possibly agricultural (Merritt 2004, personal communication). To resolve the misrepresentation of the land cover due to seasonal changes, the TFS-LC data was compared with the county crop yield and LU data to replace the barren with agriculture LU types (Byun et al., 2005).

We also added additional classes in TFS-LULC data to better represent the central part of the Houston–

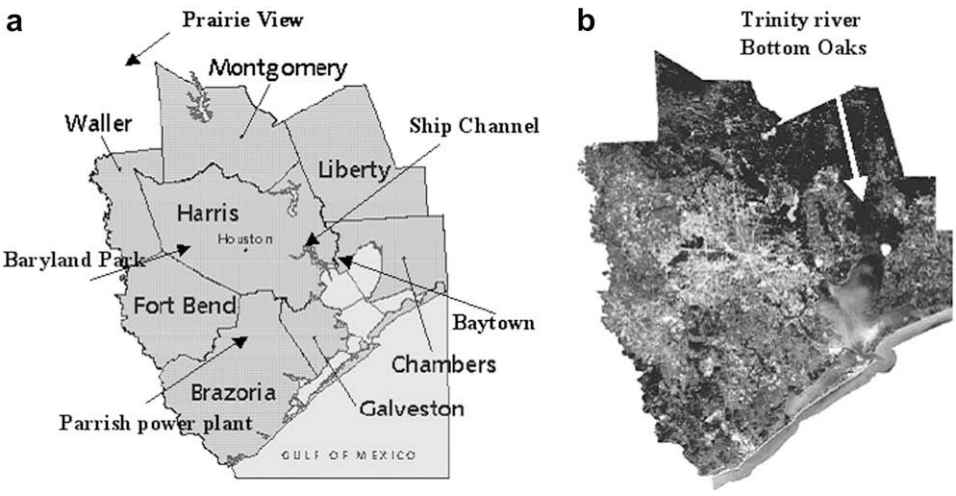

Fig. 1. (a) Study area includes Houston and surrounding eight counties, (b) is corresponding LANDSAT image (GEM, 2003).

Galveston–Brazoria (HGB) area for meteorological simulations. First, the TFS-LU residential class is used to replace all other classes except trees (broadleaf, evergreen and mixed forests) in the TFS-LC data. Second, because MM5 uses only dominant LULC class and small changes in the LULC data is not reflected in the moisture and energy budget computation, we created the residential forest land use class to represent more vegetation cover in the residential area. This class is added for cells where (1) residential is the dominant LU and (2) total forest area (broadleaf, evergreen, and mixed forests) is more than 30% of cell coverage (Byun et al., 2005).

Fig. 2a displays the dominant land use types at the 4-km resolution modeling domain derived from the USGS-LULC data for Houston and the surrounding areas. In this data, the center of Houston is represented as a large contiguous impervious surface area (represented in red), without differentiating among the urban, residential, planted trees, and road LULC types. Compared to the USGS-LULC, the TFS-LULC data resolves the single urban class in USGS-LULC into grass, trees, residential, and urban impervious surface LU types (see Fig. 2b). For the Houston Ship Channel area, where large industrial emission sources are located, USGS-LULC classifies the area as grass, but TFS-LULC correctly identifies the area as impervious surface with developed structures. The built-up structures of the airport are not represented in the USGS-LULC data but are correctly identified in the TFS-LULC data. Another noticeable difference between the two LULC datasets is that most of the dry/crop land type in the USGS-LULC is replaced with the grass type in the TFS-LULC datasets. The TFS-LULC shows more precise identification of the urban impervious surface type for the central business district (CBD), the industrial complex in the Ship Channel, and the inclusion of the residential type (which is not used in the UGSG-LULC) expanding the area of anthropogenic activities to the larger surrounding areas.

3. Model design and meteorological conditions during the event

This MM5 sensitivity study was designed to compare effects of different land use data on meteorological simulations. MM5 simulations were performed by utilizing the original USGS-LULC dataset (MM5-USGS) and by replacing the USGS-LULC with the TFS-LULC dataset (MM5-TFS) within the Houston eight county areas in the 4-km resolution domain.

The model configuration setup and physical options used are discussed below. The synoptic weather condition of the episode is also described.

3.1. Model design

This study used the MM5 Version 3 Release 6 (MM5v3.6.0) (Grell et al., 1994). The simulation period was from 22 August to 01 September 2000 as part of the TexAQS 2000 Experiment. Fig. 3 shows the model domain setup; domain 1 (D1) is at 108-km resolution covering all of North America (not shown), and domains 2–4 (D2, D3, D4) are at 36-, 12-, and 4-km resolutions, respectively. Table 1 summarizes corresponding grid configurations.

MM5 physical options applied include: Grell cumulus scheme at the 108-, 36- and 12-km resolution domains, MRF PBL scheme, Dudhia simple ice microphysical scheme, and RRTM radiation scheme. The first guess and boundary conditions were taken from the NCEP Eta model. For the first three domains the analysis nudging approach was employed for the upper-air wind, temperature and water vapor; however, the surface analysis was calculated without any nudging. The observation nudging of the profiler winds was applied for the 4-km domain. The observation nudging file was prepared by Nielsen-Gammon (2002b). The selected physical options above have been verified suitable for Houston's simulation by Nielsen-Gammon (2001).

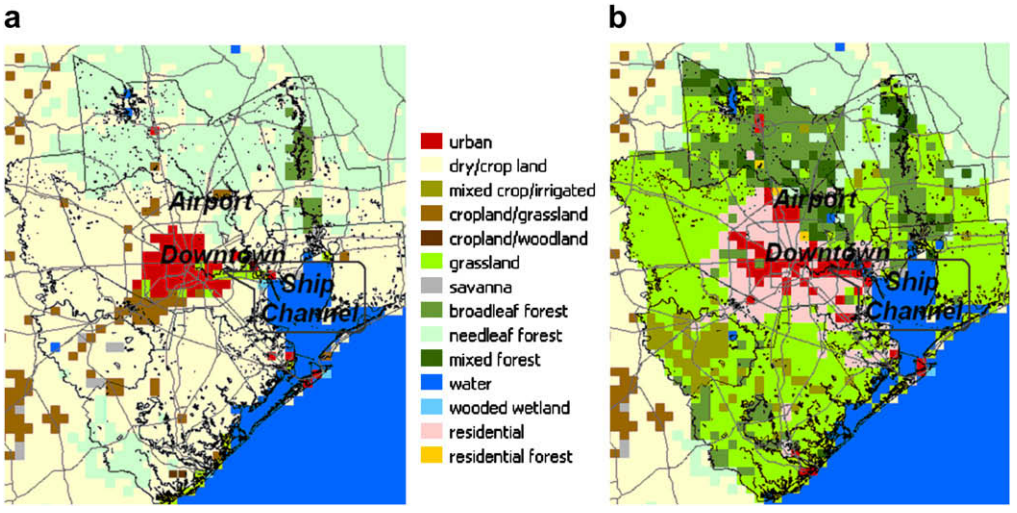

Fig. 2. Dominant land use types at 4-km resolution from (a) original USGS 25-category and (b) TFS-LULC dataset. Location of Houston downtown, Ship Channel and airport are identified; major road network is layered on top of map.

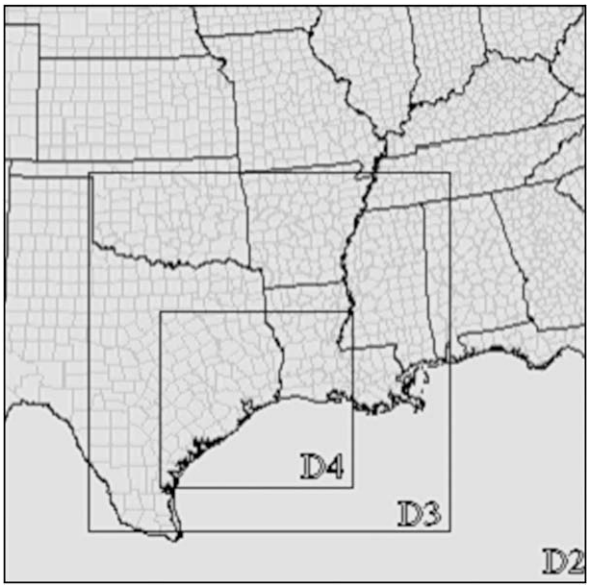

Fig. 3. Meteorological model domains: D2, D3 and D4 are at 36-, 12- and 4-km resolutions respectively.

Meteorological modeling was performed with Noah LSM (Chen and Dudhia, 2001), which incorporates detailed land surface processes such as vegetation evapotranspiration and moisture diffusion processes that are not included in the simple soil module (SLAB) (one of the land surface processes in MM5). In the SLAB soil module, the soil moisture is described only as a constant value for each dominant land use type that does not reflect the real atmospheric condition. During the TexAQS 2000 episode, the atmosphere was reported wet in the 1st half of the episode, and dry in the 2nd half of the episode. The MM5 simulation with the SLAB soil module had difficulties in simulating meteorological conditions in the HGB area under this extreme wet or dry atmospheric condition. Nielsen-Gammon (2002b) mitigated this problem by utilizing time varying soil moisture values for each land use type. In the Noah LSM, the soil moisture, after initialization with larger-scale assimilation data, is being updated with the recent precipitation/evapotranspiration prediction. The comprehensive land surface processes of Noah LSM will be necessary to represent the effects of LULC differences on the meteorological simulations.

3.2. Specification of land surface parameters

In order to accommodate the TFS-LULC data in MM5, two additional types (residential and residential forest) were introduced. The specifications of the land surface parameters for the additional types were determined through the look-up tables originally used in the meteorological modeling, the datasets for the measured albedo (GEM, 2003) and roughness length (Stetson, 2004), and the derived emissivity (GEM, 2003).

GEM (2003) generated a dataset for albedo through the direct conversion of the LANDSAT image pixels into a physical reflectance value. A principal components (PC) transformation was applied on the original LANDSAT data, and then one of the PC output files was banded to the corresponding surface reflectivity on a scale of 0–255 digital numbers (DN). The DN values were scaled to the range of the albedos used in MM5 to establish the value for the new LU types. We re-estimated the mean, median, maximum and minimum value of albedo for each LULC type from this gridded measurement dataset (see Table 2) (Byun et al., 2005). The mean value was obtained by averaging values from all the grid points with the same dominant land use type.

The emissivity was derived by GEM (2003) using the look-up tables from the meteorological modeling. We re-generated the emissivity (see Table 3) following a similar procedure as used for generating the albedo. Compared to the values in MM5 look-up table, we found that the range of the emissivity was too small to represent the corresponding land use types. Therefore, we re-scaled the mean emissivity values to have the same range as those in the MM5 look-up table. The last column of Table 3 is the re-scaled value.

For the roughness length, Burian et al. (2004) computed the value using the data from the Synthetic Aperture Radar (SAR) instrumentation (Stetson, 2004) and estimated the mean roughness length for each LULC type. Table 4 shows the mean roughness length for a few LULC types used by Burian et al. (2004). Compared to the parameter values utilized in the Noah LSM, the satellite data shows very different estimations, suggesting that different look-up tables from those used in the Noah LSM were used in the processing. To best utilize the spatial variability of the satellite estimated parameters while keeping a similar range of the parameters used in Noah for each LULC type, we have scaled the roughness lengths following the look-up table defined in the Noah LSM. The re-scaled roughness length values are listed in the last column of the Table 4.

Following the look-up table for the Noah LSM, we estimated the parametric values for the residential type to be in between the urban and grass types. For the residential forest type, the albedo was determined to be the same as

Table 1
Domain configuration

Domain	No. of cells in *x*-direction	No. of cells in *y*-direction	Z level	Resolution (km)
1	53	43	43	108
2	55	55	43	36
3	100	100	43	12
4	136	151	43	4

Table 2
Albedo recalculated from GEM (2003) measured value (mean value is used for modeling)

	LULC type	Sample	Mean	Median	Maximum	Minimum
(1)	Urban	59	0.167	0.168	0.234	0.06
(2)	Grass	631	0.168	0.168	0.239	0.035
(3)	Deciduous forest	230	0.148	0.147	0.195	0.109
(4)	Evergreen forest	62	0.143	0.143	0.163	0.126
(5)	Mixed forest	56	0.136	0.139	0.155	0.08
(6)	Residential	146	0.169	0.170	0.206	0.048
(7)	Residential forest	3	0.143	0.145	0.146	0.138

Table 3
Emissivity recalculated from GEM (2003) derived value

	LULC type	Sample	Mean	Median	Maximum	Minimum	Scaled
(1)	Urban	59	0.9828	0.984	0.99	0.974	89.83
(2)	Grass	631	0.9892	0.990	0.990	0.978	98.21
(3)	Broadleaf forest	230	0.9882	0.988	0.990	0.974	96.90
(4)	Coniferous forest	62	0.9879	0.988	0.990	0.980	96.51
(5)	Mixed forest	56	0.9879	0.988	0.990	0.980	96.51
(6)	Residential	146	0.9852	0.990	0.990	0.990	92.98
(7)	Residential forest	3	0.9833	0.988	0.988	0.974	90.49

Scaled value based on scale provided from MM5 look-up table.

the mixed-forest type, and roughness length was determined to be in between the residential and mixed-forest types. The emissivity of residential forest was determined to be close to the evergreen broadleaf forest type. The residential forest type was one of the LULC forest classes because we added for cells where (1) residential LC is dominant and (2) total forest area (broadleaf, coniferous and mixed forests) takes more than 30% of cell coverage. Thus, emissivity for the residential forest was assigned a value of 0.95, similar to deciduous broadleaf forest (0.94) and evergreen broadleaf forest (0.95). An investigation conducted by TFS showed that the dominant tree composition for the urban residential area in Houston was oak (Quercus), followed by Pinus and Sapium (Merritt 2004, personal communication). Therefore, it was assumed that the emissivity assigned for evergreen broadleaf forest would adequately represent that for residential forest.

Table 5 lists the land surface parameters utilized inside MM5 for the residential and residential forest types. Surface parameters for urban, grassland, deciduous broadleaf, evergreen broadleaf and mixed-forest types are also listed, following the look-up tables for the Noah LSM in MM5. To validate the values of residential and residential forest types in Table 5, we compared the newly assigned albedo, emissivity and roughness length for the residential and residential forest type in Table 5 with those provided in Tables 2, 3 and 4. Fig. 4 compares the spatial distribution of albedo between the re-estimated values from GEM (2003) (mean value from Table 2) (panel a) and those in Table 5 utilized inside MM5 (panel b). The spatial distributions of the two were quite similar (similar to comparisons for emissivity and roughness length plots, which are not shown in this paper). For roughness length, the values we used (Table 5) were very close to those in the last column in Table 4, which were estimated from the satellite data (Stetson, 2004).

Table 4
Z_0 is roughness length from satellite-derived value (Burian et al., 2004) and scaled Z_0 is re-scaled value based on MM5 look-up table

	Land use type	Z_0 (cm)	Scaled Z_0 (cm)
(1)	Mixed urban or built-up	62	46
(2)	Industrial	47	35
(3)	Transportation utility	41	31
(4)	Grass	16	12
(5)	Forest land	67	50
(6)	Residential	43	32

Table 5
Land surface parameters used in Noah LSM

	Land use type	Albedo	Z_0	Emissivity	$R_{c\,min}$	R_{gl}	h_s
(1)	Urban	0.18	50	0.88	200	999	999
(2)	Grass	0.19	12	0.985	40	100	36.25
(3)	Deciduous broadleaf forest	0.16	50	0.94	100	30	54.53
(4)	Evergreen broadleaf forest	0.12	50	0.95	150	30	41.69
(5)	Mixed forest	0.13	50	0.94	125	30	47.35
(6)	Residential	0.18	30	0.94	40	100	36.25
(7)	Residential forest	0.13	40	0.95	125	30	47.35

Roughness length (Z_0) is in cm, minimal stomatal resistance ($R_{c\,min}$) is in $s\,m^{-1}$, R_{gl} is visible solar flux ($W\,m^{-2}$), and h_s (unitless) is a parameter for calculating vapor pressure.

The minimum stomatal resistance, $R_{c\,min}$, is used to calculate the canopy resistance R_c, which is computed inside Noah LSM using the following formula:

$$R_c = \frac{R_{c\,min}}{LAI F_1 F_2 F_3 F_4}. \quad (1)$$

Here, LAI is the leaf area index. F_1 represents the effects of solar radiation. F_2 takes into account the effect of the water stress on the surface resistance. F_3 represents the effects of the vapor pressure deficit of the atmosphere. F_4 represents an air temperature dependence on the surface resistance. The formulations for F_1 and F_2 are given as

$$F_1 = \frac{R_{c\,min}/R_{c\,max} + f}{1 + f}, \quad (2)$$

$$F_2 = \frac{1}{1 + h_s[q_s(T_a) - q_a]}, \quad (3)$$

with $f = 0.55(R_g/R_{gl})(2/LAI)$. $R_{c\,max}$ is the maximum cuticular resistance of the leaves and is set to 5000 $s\,m^{-1}$, roughness length (Z_0) is in cm, minimal stomatal resistance ($R_{c\,min}$) is in $s\,m^{-1}$, R_{gl} is a limit value of 30 $W\,m^{-2}$ for a forest and of 100 $W\,m^{-2}$ for a cropland or grass type (Noilhan and Planton, 1989), R_g is solar radiation at the surface, h_s is a unitless coefficient for calculating vapor pressure, $q_s(T_a)$ is the saturated water vapor mixing ratio at the temperature T_a, and q_a is the mixing ratio at the surface. The F_2 function in Chen and Dudhia (2001) corresponds to the F_3 function in Noilhan and Planton (1989), where it is defined as $F_{3(Noilhan)} = 1 - g[q_s(T_a) - q_a]$ with g as a species-dependent empirical parameter similar to h_s. If h_s is very small, the definition of F_2 becomes the same as that defined in Noilhan and Planton (1989). The formulations for F_3 and F_4 are defined as

$$F_3 = 1 - 0.0016(T_{ref} - T_a)^2, \quad (4)$$

$$F_4 = \sum_{i=1}^{3} \frac{(\theta_i - \theta_w)d_{zi}}{(\theta_{ref} - \theta_w)(d_{z1} + d_{z2})}. \quad (5)$$

Chen (2005) identified that currently R_c still exhibits large uncertainties in the Noah LSM. He performed sensitivity tests to understand the effect of changes in the canopy resistance on the simulated flux components and found out that typically, when $R_{c\,min}$ changed by a factor of 4 (from 30 to 120 $s\,m^{-1}$), the energy fluxes were changed

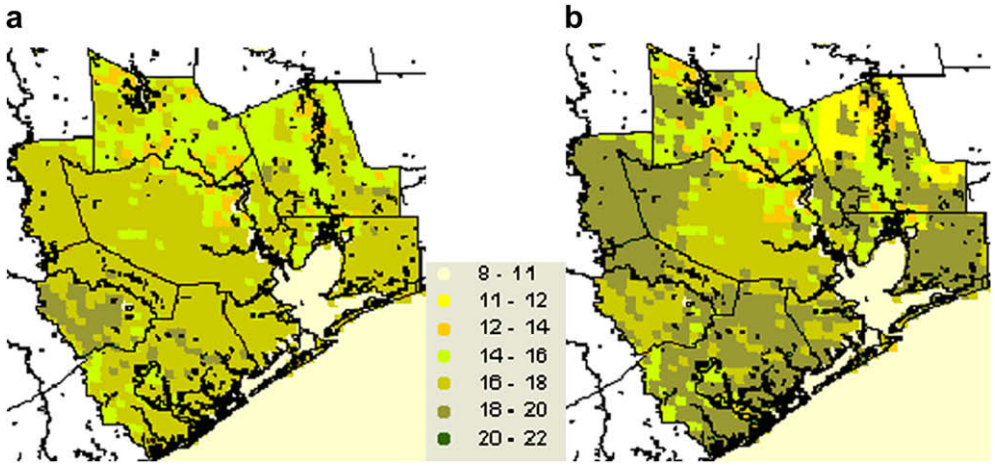

Fig. 4. Spatial comparison of albedo (%) between (a) re-estimated values from GEM (2003) (mean value from Table 2) and (b) values in MM5 (Table 5). There is no data outside the eight county areas except for the water body.

by a factor of 2. Based on the information developed above, $R_{c\ min}$, R_{gl} and h_s for the residential LULC type are set equal to those for the grass type; for the residential forest, they are set equal to the mixed-forest type in this study. A series of MM5 sensitivity tests were performed with various combinations of parametric values and the results were compared with measurements (mostly temperature and wind). Through these comparisons, it was confirmed that the parametric values used in this study were suitable to represent Houston's surface characteristics.

3.3. Synoptic weather conditions

The synoptic conditions of the episode were summarized from Nielsen-Gammon (2002a). In this paper, we focused on the analysis from 25 to 30 of August 2000. On 25 August, the land breeze was dominant in the early morning, and then the flow became stagnant and changed directions from offshore to onshore flow when the sea breeze developed in the early afternoon (1300 CST). Skies were clear to partly cloudy in Houston. On 26 August, winds changed from northwesterly, westerly, then to southerly in the morning (0800–1000 CST). By 1400 CST, winds became southeasterly everywhere, and then they strengthened during the remaining hours. On 27 August, the winds were similar to the previous day. The southeasterly winds continued on 28 August, then slowly veered to a southwesterly flow during the night (0000–0400 CST), and turned to a northeasterly flow in the early morning (0700 CST). By 1000 CST, winds reversed direction and became southwesterly, and then veered to southeasterly by 1300 CST. The southeasterly winds continued for the remainder of the day. On 29 August, the westerly winds dominated the general flow until 1400 CST, and then southerly to southeasterly winds developed. The sky was clear in the Houston area. Temperatures were higher than the previous days. On 30 August, the nighttime winds were westerly, and then continued veering into northwesterly and strengthened until midday. In the following hours, the offshore flow became weak in Houston and winds became southerly and southeasterly at the onset of the sea breeze (1600 CST). Maximum temperatures recorded were above 40 °C in several continuous ambient monitoring station (CAMS) surface sites. Some shower activities were present on 25 (in the late afternoon near Liberty), 27 (in the morning south of Houston), and 31 of August (in the mid afternoon in the Beaumont area).

4. MM5 simulation problems

The initial MM5 simulations with Noah LSM and a selected set of physical options presented a few problems.

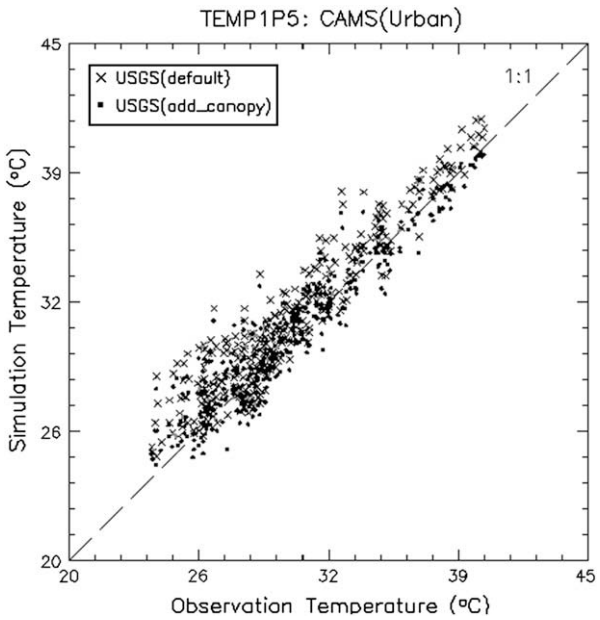

Fig. 5. Scatter diagram of air temperature from CAMS measurement sites and MM5 simulations in urban areas. (Cross mark is simulation using original Noah LSM, and dot mark is simulation with added canopy water amount.)

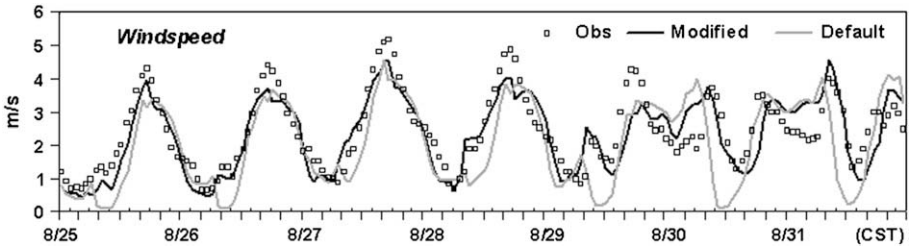

Fig. 6. Time series comparison of averaged wind speed from CAMS sites and simulation outputs. (Rectangle mark: observation, black line: MM5 simulation with modified MRF code, gray line: regular MM5 simulation).

In this section, we address the modifications made to improve the simulations.

4.1. Noah LSM with USGS-LULC

The MM5 simulation with USGS-LULC data overestimated daytime temperatures. To compute the land surface processes, the Noah LSM uses the dominant land use class resolved from the 1-km resolution USGS-LULC data. With the dominant land use classification, the Houston metropolitan area is shown completely as the urban impervious surface type. However, the detailed LULC map from the TFS shows that at least 20% of the area is covered with trees and vegetation. This leads to the question, "How can we represent evapotranspiration processes in the Houston urban area with the USGS-LULC data?" Nielsen-Gammon (2002b) overcame the difficulties by changing the daily values of soil moisture with the 5-layer slab land surface module in MM5. However, inspection of the Noah LSM codes revealed that the change of the soil moisture values in the urban substrate would not correct this problem because the urban land surface was treated as the impervious surface type. The high surface resistance values assigned for the urban land use category effectively blocked transfer of any mass, including moisture from the soil to the atmosphere (and vice versa) (Cheng et al., 2003), and therefore could not account for the urban vegetation effects.

In the Noah LSM, the intercepted canopy water content is computed with

$$\frac{\partial W_c}{\partial t} = \sigma_f P - D - E_c, \tag{6}$$

where W_c is the intercepted canopy water content (mm), σ_f is the green vegetation fraction, P is the input total precipitation and E_c is the canopy evaporation rate

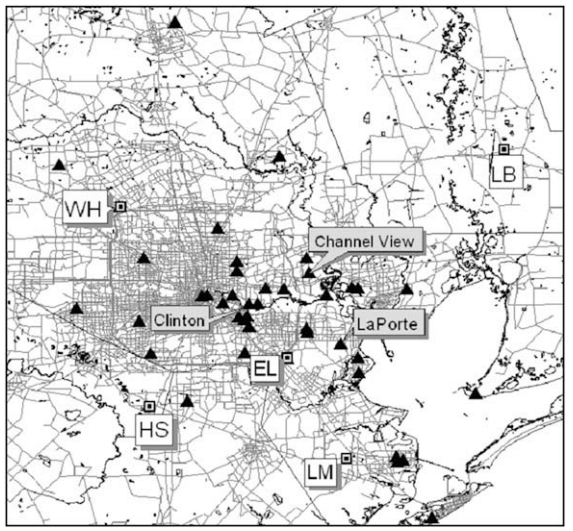

Fig. 7. Locations of CAMS (triangle mark) and wind profiler sites (WH, EL, HS, LM and LB).

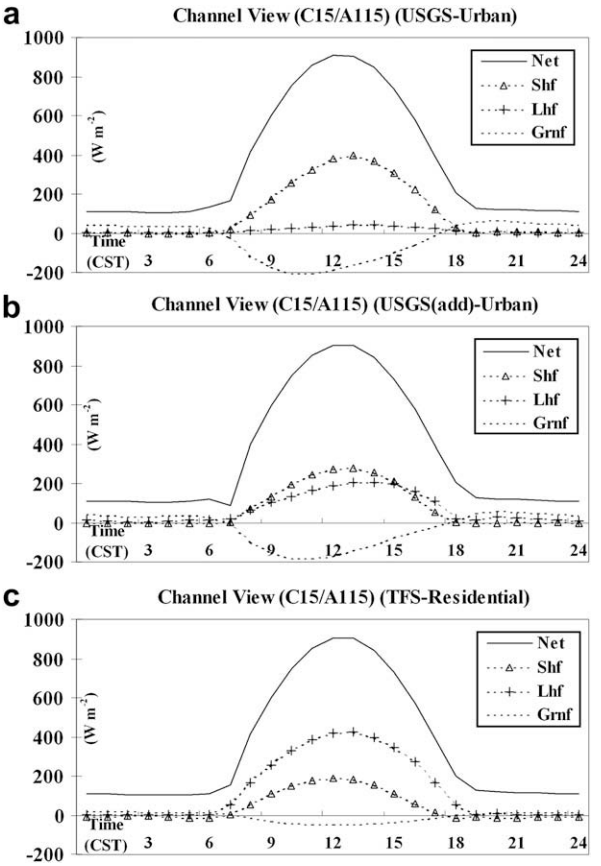

Fig. 8. Time series of flux components from MM5 simulations on 30 August of 2000 using (a) USGS (without adding canopy water), (b) USGS (adding canopy water), and (c) TFS-LULC data (Net: incoming solar radiation; Shf: sensible heat flux; Lhf: latent heat flux and Grnf: ground heat flux).

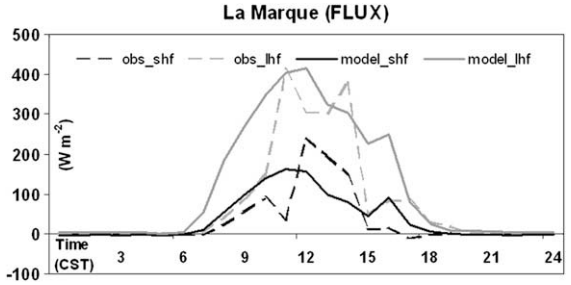

Fig. 9. Time series comparison of flux components between observation and MM5 simulations using TFS-LULC data on 22 July 2005 (black dashed line: observed sensible heat flux, gray dashed line: observed latent heat flux, black solid line: modeled sensible heat flux, gray solid line: modeled latent heat flux).

($\mathrm{mm\,s^{-1}}$). If W_c exceeds S (maximum canopy capacity: 0.5 mm), the excess precipitation or drip, D reaches the ground (Chen and Dudhia, 2001).

In order to have the vegetation transpiration effect from Houston's trees and other vegetation, a new term E_u was added to represent the anthropogenic contribution of the canopy water content in the urban area:

$$\frac{\partial W_c}{\partial t} = \sigma_f P - D - E_c + E_u. \quad (7)$$

For Houston urban areas, which include about 20% vegetation, we selected $E_u = 3 \times 10^{-6}$ ($\mathrm{mm\,s^{-1}}$) after several sensitivity simulations. Fig. 5 demonstrates the warm bias of surface air temperatures predicted by the standard MM5-Noah version released (cross mark). With the addition of the anthropogenic canopy water flux in the urban cells, the problem of high bias of the maximum temperature can be reduced (dot mark). Here, we presented solutions to reduce the high temperature bias when the USGS data was used for MM5 simulation, but the amount of canopy water needed would vary depending on the real atmospheric conditions. A more fundamental approach would be to utilize a better LULC dataset that represents land surface features accurately.

It is expected that the artificial addition of the anthropogenic canopy water is not necessary for the MM5 simulation using TFS-LULC data due to the detailed and correct representation of the land surface features (trees, grassland and residential) that exhibit the evapotranspiration and moisture diffusion processes.

4.2. Daytime wind bias

The MM5 simulation showed a problem of a 1–2 h delay in the development of daytime wind peaks, as reported in several research articles (ATMET, 2003; Cheng et al., 2004).

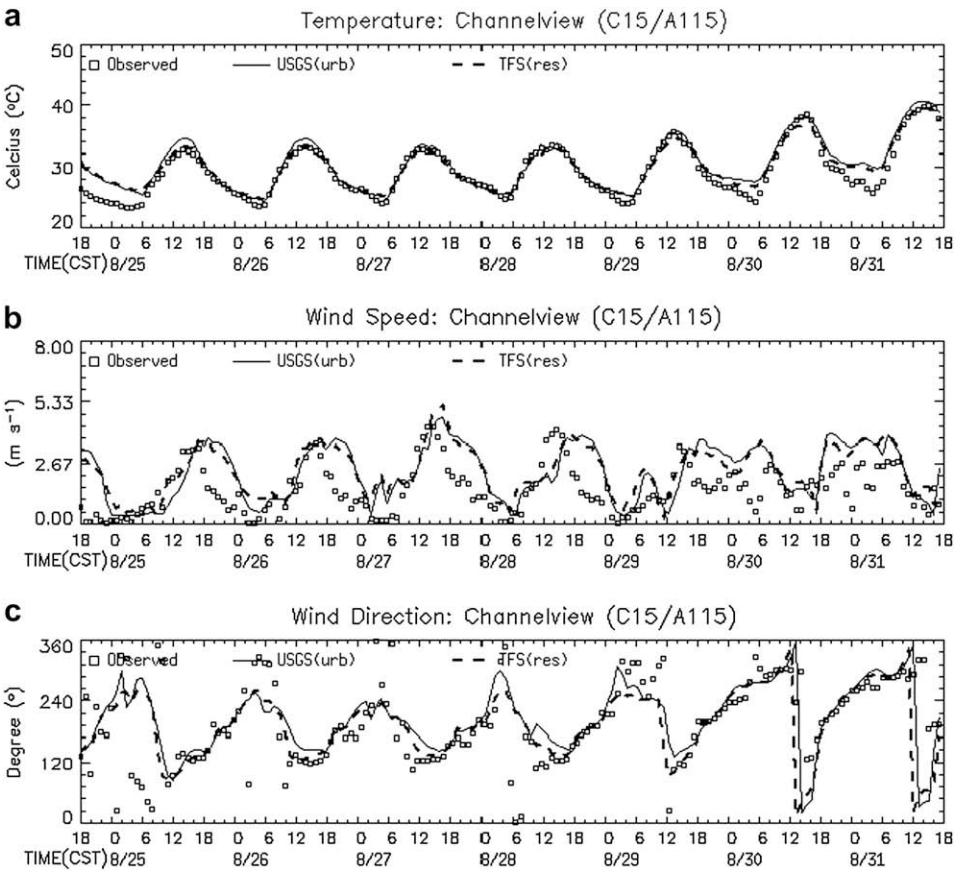

Fig. 10. Time series comparison of surface (a) temperature, (b) wind speed and (c) wind direction from MM5 simulations using USGS (solid line), TFS (dashed line) and surface CAMS measurement sites (rectangles) at Channel View site.

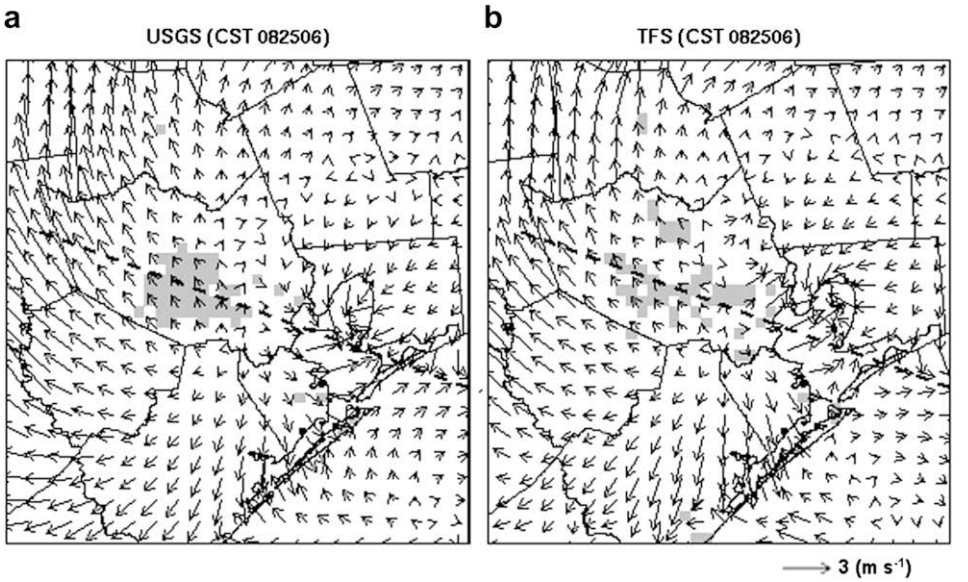

Fig. 11. Horizontal surface wind distribution from 4-km MM5 simulations at 0600 CST 25 August 2000 using (a) USGS, (b) TFS-LULC data (background color is urban land use type).

The delay was probably caused by the use of the total wind speed, unrealistically enhanced with the convective velocity component, to calculate the friction velocity in the MRF PBL scheme (Hong and Pan, 1996). In particular, at the time of rapid growth of PBL, the high momentum brought down from the free atmosphere was excessively dissipated by the enhanced friction velocity.

To resolve this problem, the MRF PBL scheme was modified to utilize the original wind speed (U), for computing the momentum flux but utilize the convective velocity (W_*) enhanced wind speed (U_e) for computing the heat flux exchange (Liu et al., 2004):

$$U = \sqrt{(u^2 + v^2)}, \tag{8}$$

$$U_e = \sqrt{\left(U^2 + \alpha W_*^2\right)}. \tag{9}$$

α, the convective enhancement factor, is set at 1.5. Fig. 6 compares wind speed time series between the observational data and the model simulations with default and modified MRF PBL schemes. With the use of more realistic representations for calculating the flux components, the diurnal evolution pattern of wind speed was improved.

5. Result of meteorological simulations

The results of the MM5 simulations were evaluated with the surface observations and wind profiler data. Fig. 7 plots the locations of the available CAMS sites (triangle mark)

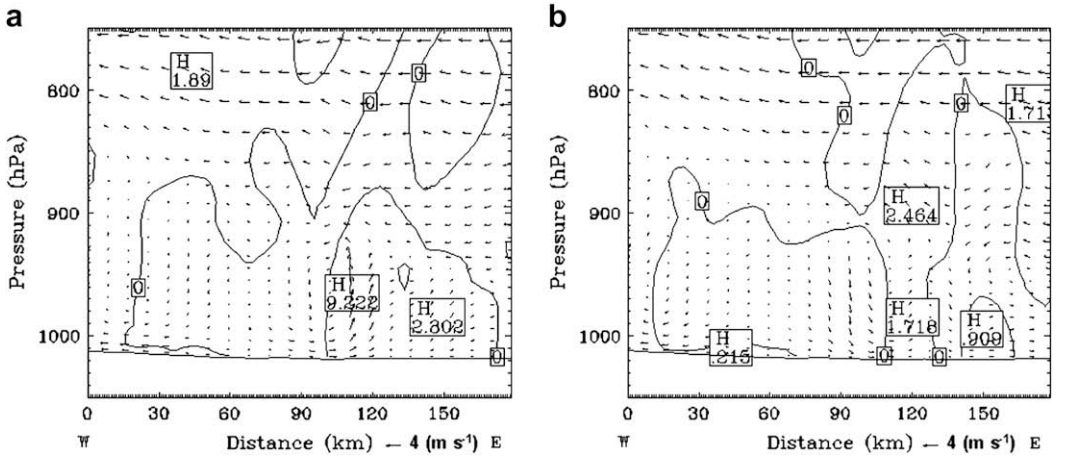

Fig. 12. Vertical cross-section plot of u, w vectors along the line shown in Fig. 11 (black dashed line) from (a) MM5-USGS and (b) MM5-TFS simulations at 0600 CST 25 August 2000 (contour line is vertical wind speed ($cm\,s^{-1}$)).

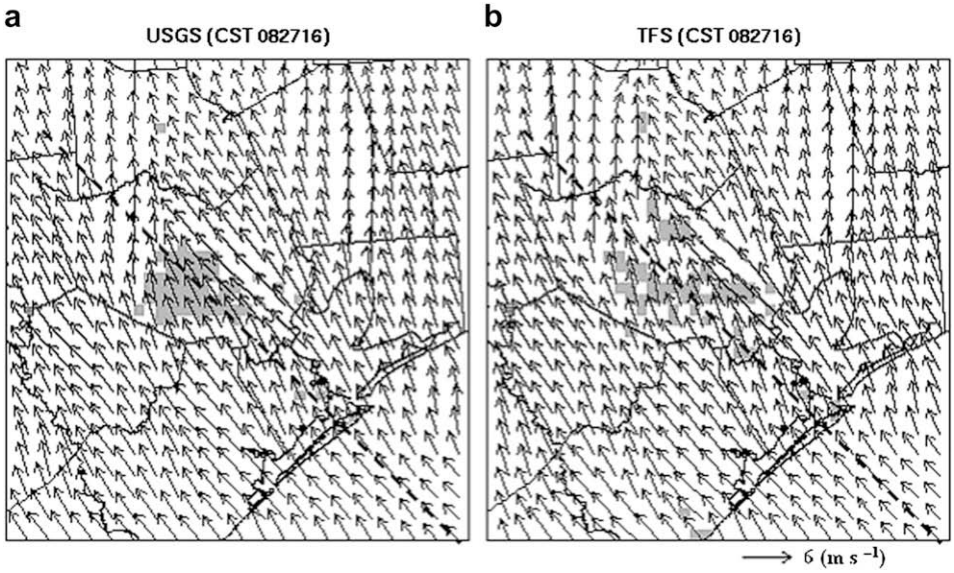

Fig. 13. Horizontal surface wind distribution from 4-km MM5 simulations at 1600 CST 27 August 2000 using (a) USGS, (b) TFS-LULC data (background color is urban land use type).

and five wind profiler sites (square mark): Liberty (LB), La Marque (LM), Ellington (EL), Wharton Power Plant (WH) and Houston Southwest Airport (HS). The CAMS sites provide the observed surface wind and temperature. The wind profilers provide the mixed layer depth retrieved from backscatter data (Senff et al., 2002). The surface flux components were also compared between model simulations.

5.1. Time series comparison of flux components, temperature and wind

Fig. 8 compares time series of flux components on 30 August of 2000 from different MM5 simulations at the Channel View site (115) (see Fig. 7 for the site location). Panel (a) is for the USGS data without adding canopy water in the urban cell; panel (b) is for the USGS data but with the added canopy water in the urban cells; panel (c) is for the TFS-LULC data. The land use type is changed from the urban in the USGS data into the residential type in the TFS data. The MM5-USGS simulation without added canopy water shows a high sensible heat flux (dashed line with triangle mark) and very low latent heat flux (dashed line with cross mark) distribution (Fig. 8a). The solid line represents the net radiation and the dashed line is the ground heat flux. After adding the canopy water in the urban cells (Fig. 8b), the net radiation is partitioned more into the latent heat flux, causing a reduction in sensible heat flux. The MM5 simulation using the TFS-LULC data characterizes this site as a residential area and the

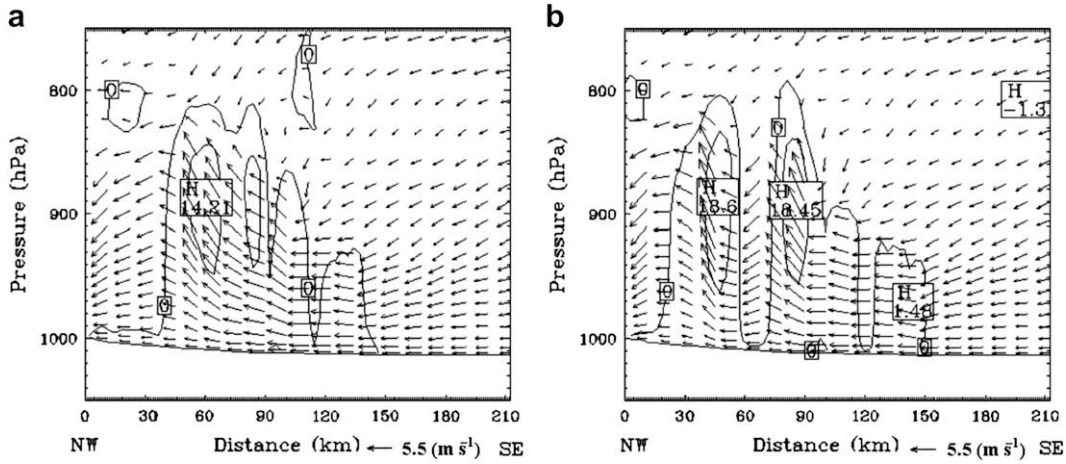

Fig. 14. Vertical cross-section plot of u, w vectors along the line shown in Fig. 13 (black dashed line) from (a) MM5-USGS and (b) MM5-TFS simulations at 1600 CST 27 August 2000 (contour line is vertical wind speed ($cm\,s^{-1}$)).

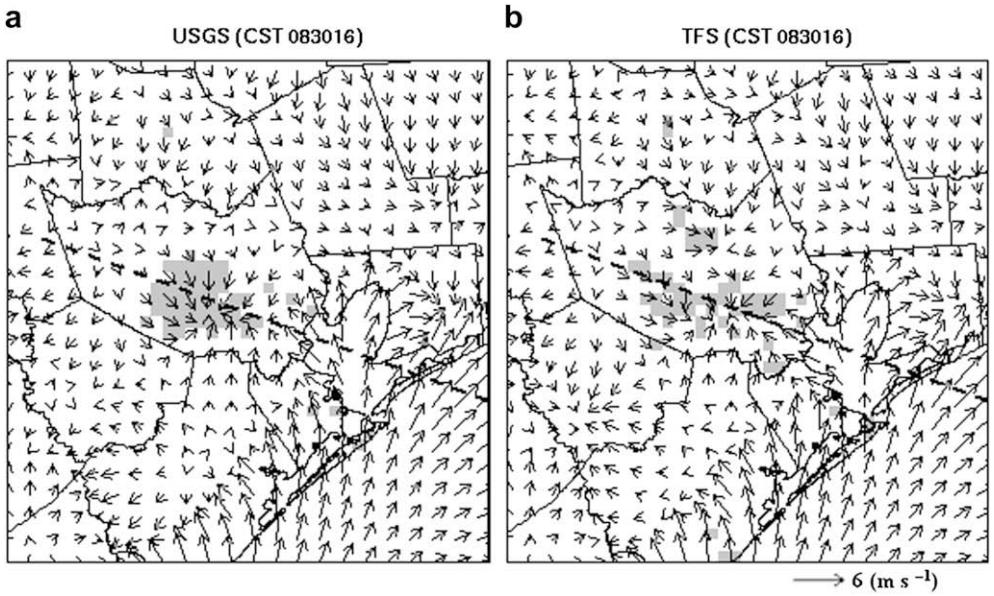

Fig. 15. Horizontal surface wind distribution from 4-km MM5 simulations at 1600 CST 30 August 2000 using (a) USGS, (b) TFS-LULC data (background color is urban land use type).

simulation results in higher latent heat fluxes (Fig. 8c). Unfortunately, there was no flux measurement in the Houston urban type area; the only flux data available for the TexAQS 2000 was from another site (La Porte) located in the sub-urban area. After consulting with the scientists in charge of the measurement data, it was determined that the data was not suitable for the present study. For this reason, we compared with the flux data measured during a 2005 episode at the University of Houston Coastal Center (UHCC), La Marque, Texas (see Fig. 7 for site location). Fig. 9 compares the sensible heat and latent heat fluxes between the observation and the model simulation using the TFS-LULC data for 22 July 2005. At the La Marque site, the observed latent heat flux was higher than the sensible heat flux, and the modified MM5 model was able to capture the general diurnal variation. The simulation for the UHCC using USGS-LULC data was also similar to this result because the land use type (grass) was the same.

Fig. 10 shows the time series comparison of the surface parameters (a) air temperature, (b) wind speed, and (c) wind direction from the MM5-USGS (without adding canopy water) and MM5-TFS simulations and measurement data at the Channel View site. The MM5-USGS simulation showed warm bias in the daytime temperature (solid line) at the site on 25, 26, and 31 of August 2000. The bias was reduced in the MM5-TFS simulation. Wind speed and direction showed substantial changes as well. The time

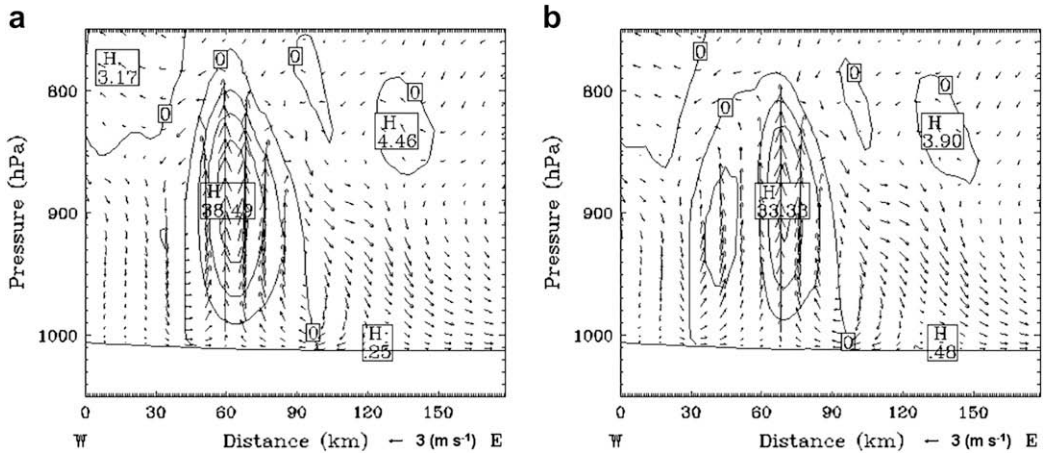

Fig. 16. Vertical cross-section plot of *u*, *w* vectors along the line shown in Fig. 15 (black dashed line) from (a) MM5-USGS and (b) MM5-TFS simulations at 1600 CST 30 August 2000 (contour line is vertical wind speed ($cm\,s^{-1}$)).

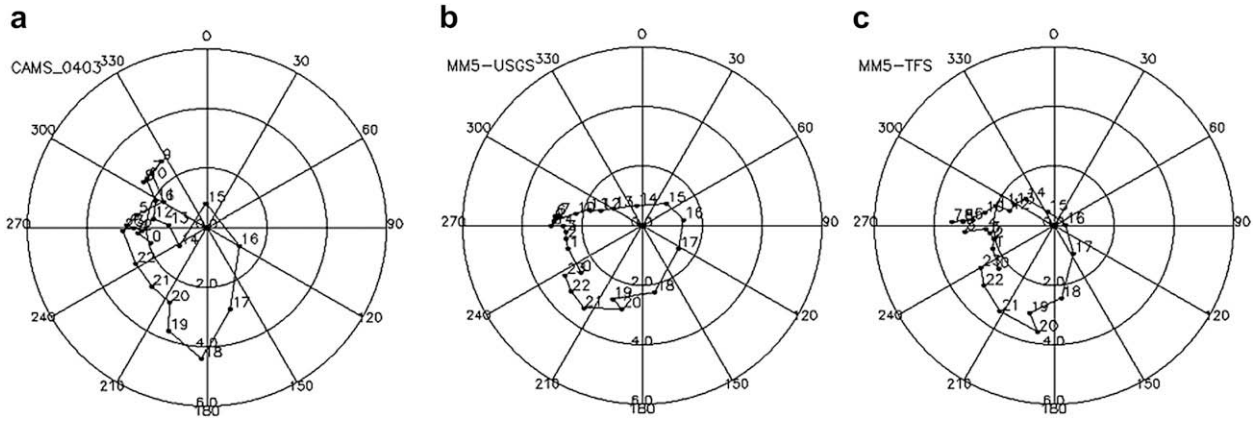

Fig. 17. Hodograph comparison at Clinton site (CAMS 403) on 30 August 2000: (a) is from measurement, (b) is from MM5-USGS simulation and (c) is from MM5-TFS simulation.

series comparison demonstrates that the change of the land use type modified the components of the energy distribution, which in turn, affected the surface temperature and wind predictions.

5.2. Horizontal and vertical wind

Difference in the LULC data also modifies flow patterns. In particular, under weak synoptic conditions, local circulation is easily affected by changes in land surface characteristics. In this section, wind flow patterns on 25, 27, and 30 of August were compared. These three days exhibited distinct flow characteristics.

5.2.1. August 25

Fig. 11 is the spatial plot of the horizontal wind vector at 0600 CST 25 August 2000 from (a) MM5-USGS and (b) MM5-TFS simulations; the background gray color represents the dominant urban LU type from each corresponding LULC dataset. Near the coastal area both simulations showed the offshore land breeze flows, while inside the City of Houston, the flow patterns were modified according to the distribution of the urban LU type. The MM5-USGS simulation featured southerly wind components over the urban area and stronger wind speed than the MM5-TFS simulation.

Vertical cross-sections of the wind vectors are analyzed along the line crossing the Gulf of Mexico, Galveston Bay and the Houston downtown area (dashed line in Fig. 11). Fig. 12 shows the $\tilde{u}$ and $\tilde{w}$ wind components ($\tilde{u}$: the wind vector along the cross-section line, $\tilde{w}$: the vertical wind also shown as the contour line) at 0600 CST 25 August from MM5-USGS (Fig. 12a) and MM5-TFS (Fig. 12b) simulations. Both simulations showed similar upper level flow patterns, but near the surface MM5-USGS shows a better defined land breeze return flow structure over the Galveston Bay area than in the MM5-TFS simulation.

5.2.2. August 27

Fig. 13 is the spatial plot of the horizontal wind vector and Fig. 14 is $\tilde{u}$ and $\tilde{w}$ wind components at 1600 CST 27 August 2000. Unlike 25 August, on 27 August the flow was dominated by a strong southeasterly wind; therefore, the local circulations did not differ much between the two

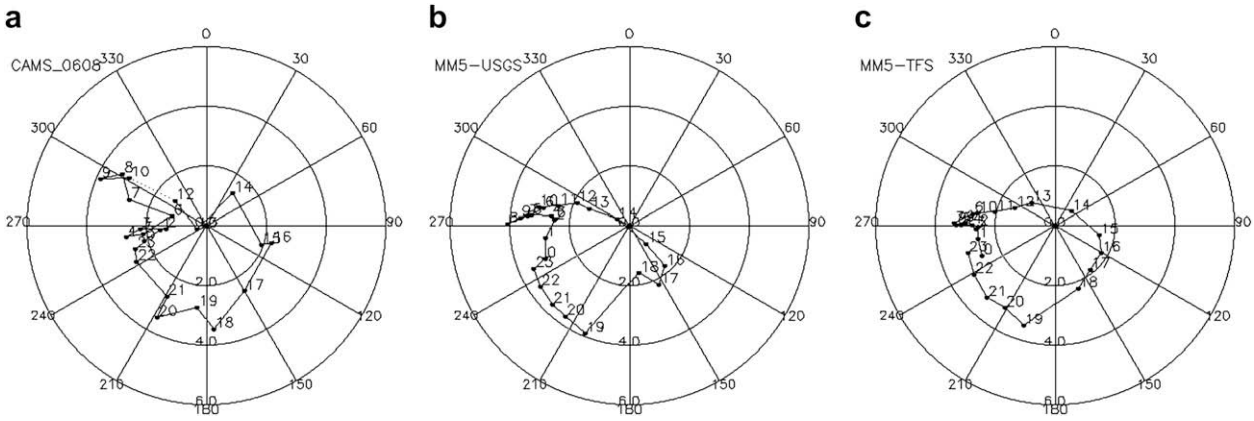

Fig. 18. Hodograph comparison at La Porte site (CAMS 608) on 30 August 2000 (CST time): (a) is from measurement, (b) is from MM5-USGS simulation and (c) is from MM5-TFS simulation.

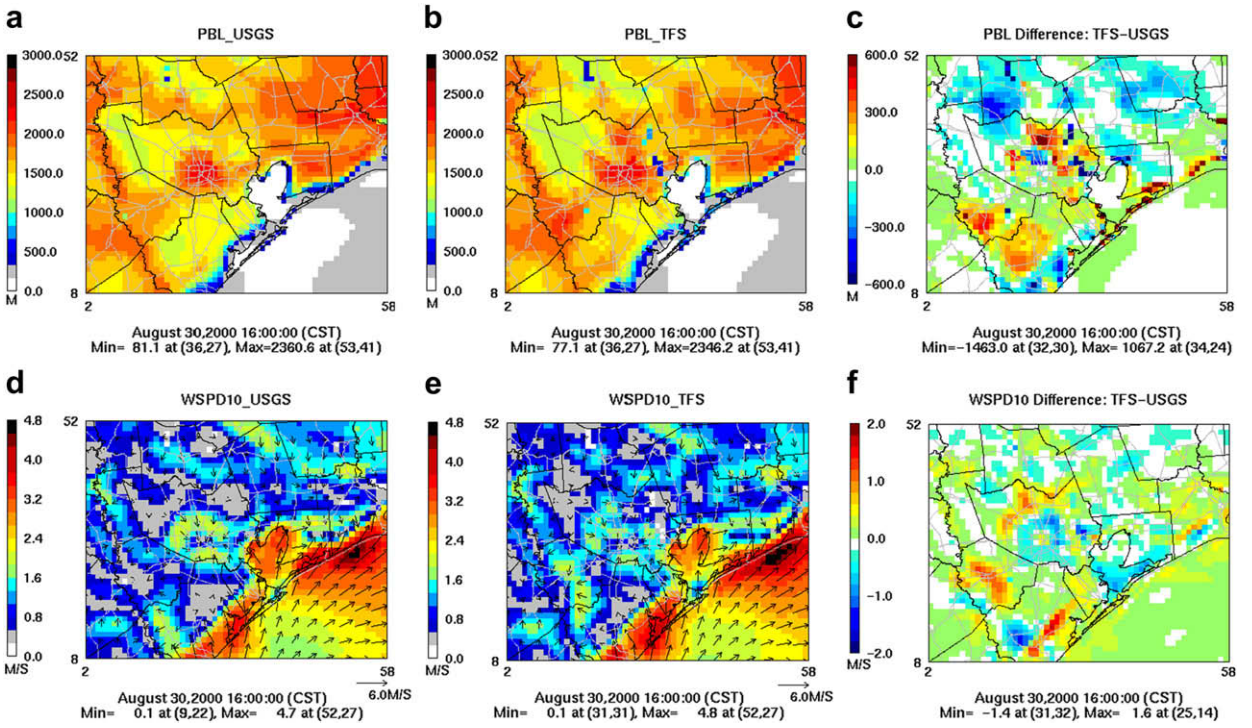

Fig. 19. Spatial plot of PBL height from (a) MM5-USGS, (b) MM5-TFS simulations and (c) is PBL difference plot, (d) and (e) are wind speed and vector (m s^{-1}) from MM5-USGS and MM5-TFS simulations, respectively, (f) is wind speed difference plot at 1600 CST 30 August 2000.

MM5 simulations. We generated a vertical cross-section plot crossing the Gulf of Mexico and the Houston downtown area (dashed line in Fig. 13). Strong southeasterly winds dominated over all layers showing similar flow patterns between the two MM5 simulations except in the Houston urban area, where the convective activity changed due to the difference in the urban land use distribution.

5.2.3. August 30

Fig. 15 is the spatial plot of the horizontal wind vector and Fig. 16 is $\tilde{u}$ and $\tilde{w}$ wind components at time 1600 CST 30 August 2000. On this day, the ambient winds showed an offshore flow until the time of the sea breeze onset (Banta et al., 2005). Both simulations captured the onshore sea breeze flow and the sea breeze fronts were clearly observed. The wind flow patterns were modified in accordance with the LU distribution between the MM5-USGS and MM5-TFS simulations. The location of the convergent zone in MM5-USGS simulation (Fig. 15a) corresponded to the specification of dominant urban type. In the MM5-TFS simulation (Fig. 15b), the strength of the convergent flow was reduced. The wind was very stagnant in the Houston downtown and Ship Channel area. The vertical cross-section plot along the same line as in Fig. 11 shows that the large impervious urban area in the USGS-LULC data induced stronger convective activity (Fig. 16a) than in the MM5-TFS simulation (Fig. 16b) in the Houston downtown area. In the upper air, the ambient winds were still offshore, but near the surface, the onshore sea breeze flows developed.

5.3. Hodograph

Fig. 17 is the hodograph comparison at the Clinton site (CAMS 403), located near the Ship Channel emission source area (see Fig. 7 for site location) on 30 August. At the Clinton site, winds were dominated by westerly to northwesterly flows during the night and morning hours; there was a clockwise turn to south to southwest directions with the onset of the onshore sea breeze flow (Fig. 17a). The MM5-USGS simulation (Fig. 17b) showed a clockwise turn but produced an overly strong northeast component in the early afternoon (CST 1400–1600), as well as depicted the weak onshore southerly wind. The wind bias could be attributed to the complete urban impervious surface type specified that generated a stronger convergence flow in the Houston downtown area. The MM5-TFS simulation (Fig. 17c) did a better job of capturing the wind turning and the magnitude of the wind speed than MM5-USGS simulation, although the timing was slightly off.

Fig. 18 is the hodograph comparison on 30 August at La Porte site (CAMS 608), located near the Galveston Bay area, which is often influenced by the bay breeze flow (see Fig. 7 for the site location). Neither simulation captured the northwest wind in the early morning (CST 0700–1000). The MM5-USGS simulation failed to produce a northeast wind in the early afternoon (CST 1400), while the MM5-TFS simulation did capture the northeast component. The MM5-USGS simulation generated too weak southeasterly onshore sea breeze flows and too strong southwesterly flows, while the MM5-TFS simulation showed the same

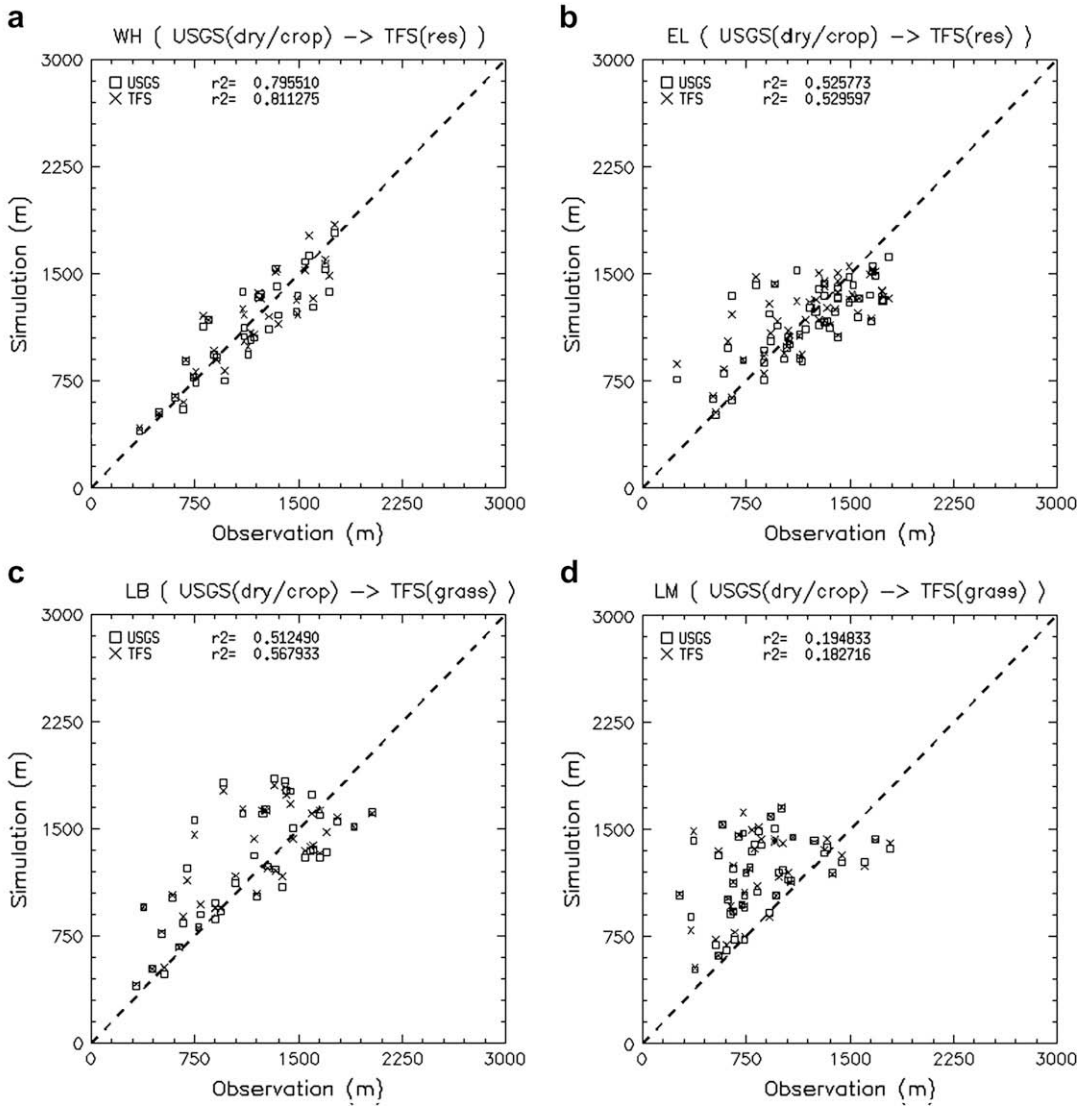

Fig. 20. Scatter diagram of PBL height from wind profiler data and model simulations: MM5-USGS (square mark), MM5-TFS (cross mark) at (a) WH, (b) EL, (c) LB and (d) LM sites.

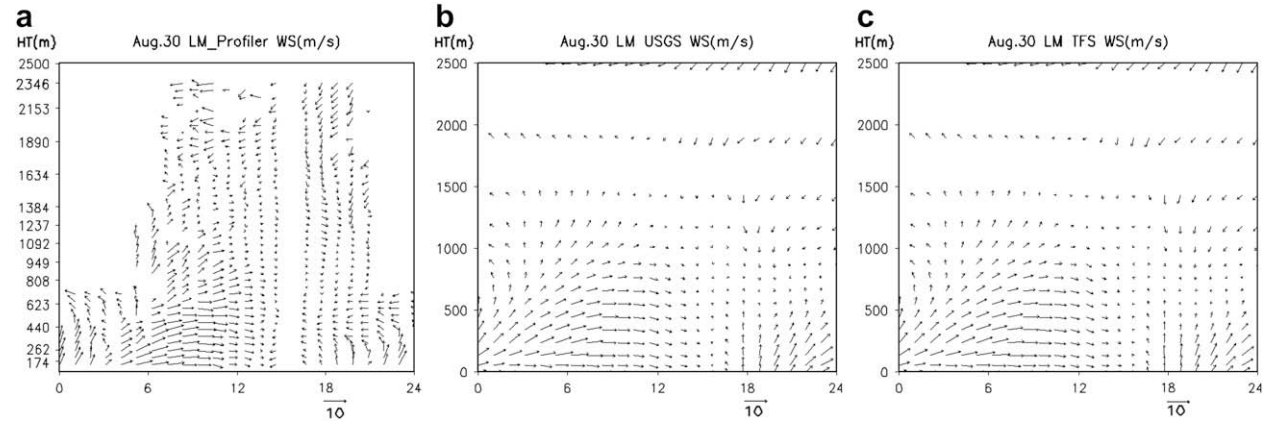

Fig. 21. Comparison of wind speed and vector from (a) wind profiler data, (b) MM5-USGS and (c) MM5-TFS simulations at LM site on 30 August (CST time).

pattern but with less bias than the MM5-USGS simulation. The wind direction change from offshore to onshore flow (CST 1400–2000) was well simulated in the MM5-TFS simulation.

5.4. PBL height and wind distribution

Fig. 19 compares the spatial distribution of the PBL heights at 1600 CST 30 August 2000 from the MM5-USGS (panel (a)) and MM5-TFS (panel (b)) simulations, and the difference plot (panel c). Panels (d) and (e) show the wind vector and speed from the MM5-USGS and MM5-TFS simulations respectively, and the difference plot (panel (f)). The distribution of the PBL height was consistent with the land use types; in the Houston downtown area, deeper PBL heights were predicted in the places where the urban impervious surface type was specified. The MM5-USGS simulation showed stronger wind speeds in the Houston downtown area than the MM5-TFS simulation, which showed more stagnant wind conditions. The MM5-USGS simulation (Fig. 19a) showed the characteristic but unreal urban heat island dome in the Houston downtown area, which in turn caused stronger bay breeze flows (Fig. 19d) than those in the MM5-TFS simulation (Fig. 19e). The location of the sea breeze front penetrated deeper in the MM5-TFS simulation (Fig. 19e), which could be attributed to the overall modifications of the regional scale wind pattern and surface heat distributions due to the LULC changes within the eight county areas. Another noticeable difference was in the Houston Ship Channel area, where the cell was classified as a water body in the TFS-LULC data (refer to Fig. 2), thus producing a shallower PBL than in the surroundings (Fig. 19b). The Houston Ship Channel area has very complicated land use patterns. The TFS-LULC map represents this area as a major impervious concrete surface surrounded by a water body. Due to the fact that there are enormous emission sources located in the Ship Channel area, the correct description of the land use distribution in this area is critically important to capture the pollutant behavior affected by the local wind transport and mixing height characteristics.

5.5. Comparison with wind profiler data (PBL height and wind speed)

Fig. 20 is a scatter diagram comparing PBL heights for the 7-day period (25–31 of August) from the two MM5 simulations and the wind profiler data (the R^2 values are shown in the figure). The mixed layer heights estimated by the wind profiler measurements were collected from five profilers located at La Marque (LM), Houston Southwest (HS), Ellington Field (EL), Wharton (WH), and Liberty (LB) (Senff et al., 2002). Since the land use types at the profiler sites were similar in both USGS- and TFS-LULC, the difference in MM5 at these sites was not obvious. The LULC differences (from dry/crop land in USGS data to residential type in TFS data) at the WH and EL sites (Fig. 20a and b) resulted in a slight increase in the predicted PBL heights in the MM5-TFS simulation. Both simulations over-predicted the PBL heights at the LB and LM sites (Fig. 20c and d) where the LULC change was from the dry/crop land type to the grassland type. Site LM was located near the coastline and was influenced by the shallow marine boundary layer, where both simulations failed to predict the shallow PBL heights.

Fig. 21 is the wind speed comparison at LM site on 30 August. Fig. 21a is from the wind profiler data. The westerly wind was prevailing through the night near the surface layers and both simulations captured the general flow quite well. In the early afternoon, the wind was stagnant, and then the offshore flow changed into the onshore sea breeze flow. Both MM5 simulations are able to capture the onshore sea breeze flow. Differences are not apparent between the two simulations because the dry/crop and grass LULC types have similar physical characteristics in LSM.

Table 6
RMSE, mean difference and R^2 value for surface temperature and wind speed based on hourly value from 41 CAMS stations in HGB area on 25, 27 and 30 of August

Date	Sample	Statistics	Temperature		Wind speed	
			USGS	TFS	USGS	TFS
0825	525 (Temperature); 499 (wind speed)	Mean diff	0.292	0.579	0.053	0.016
		RMSE	1.543	1.525	0.940	0.880
		R^2	0.990	0.991	0.619	0.629
0827	550 (Temperature); 496 (wind speed)	Mean diff	−0.745	−0.473	0.456	0.310
		RMSE	1.400	1.202	1.059	0.975
		R^2	0.993	0.994	0.701	0.715
0830	549 (Temperature and wind speed)	Mean diff	0.083	0.407	0.432	0.341
		RMSE	1.536	1.480	1.083	1.055
		R^2	0.990	0.992	0.458	0.460

Table 7
RMSE, mean difference and R^2 value for surface temperature and wind speed from selected CAMS sites for 7-days (25–31 August 2000) episode

CAMS	Sample	Statistics	Temperature		Wind speed	
			USGS	TFS	USGS	TFS
Clute (C11)	169	Mean diff	−0.904	0.364	−0.986	−0.905
USGS: dry/crop		RMSE	1.605	1.247	1.506	1.343
TFS: urban		R^2	0.859	0.844	0.286	0.297
Kirkpatrick (C404)	169	Mean diff	−1.335	−0.828	0.148	0.017
USGS: urban		RMSE	1.817	1.504	0.814	0.819
TFS: urban		R^2	0.91	0.90	0.53	0.51
Milby Park (A169)	169	Mean diff	0.548	0.325	0.296	0.126
USGS: urban		RMSE	1.285	1.215	0.936	0.838
TFS: residential		R^2	0.925	0.927	0.523	0.580
HRM-3 (C603)	169	Mean diff	−1.41	0.28	0.073	−0.017
USGS: dry/crop		RMSE	1.854	1.504	0.941	0.925
TFS: urban		R^2	0.928	0.895	0.53	0.512
HRM-4 (C604)	169	Mean diff	0.285	0.695	0.002	0.323
USGS: dry/crop		RMSE	1.510	1.842	1.147	1.1
TFS: grass		R^2	0.915	0.906	0.362	0.430
Deer Park 2 (C35)	167	Mean diff	−0.664	0.07	0.281	0.089
USGS: dry/crop		RMSE	1.15	1.028	1.014	0.866
TFS: residential		R^2	0.94	0.93	0.50	0.534
HRM-11 (C611)	169	Mean diff	−0.37	−0.675	0.826	0.606
USGS: dry/crop		RMSE	1.243	1.436	1.183	1.015
TFS: forest		R^2	0.913	0.903	0.308	0.231

5.6. Statistical evaluation

Table 6 lists the root mean square error (RMSE), mean difference, and R^2 value based on the hourly values of 41 CAMS measurements in the HGB area on 25, 27 and 30 of August. Among the three days, 27th had the least complex wind flow patterns and the models showed the best agreement for both MM5-USGS and MM5-TFS. The diurnal variations of the temperature and wind speed were minimal due to the dominance of the regional scale flows. Overall, the MM5-TFS simulation performed slightly better than the MM5-USGS simulation. In terms of surface temperature, both models performed quite well: the R^2 values were close to 0.99, showing high correlation between model and observation, and the MM5-TFS simulation showed only slight improvement for each individual day. In terms of surface wind speed, the statistical analysis for each individual day showed improvements in the MM5-TFS simulation.

Table 7 shows the same statistics as in Table 6 but for the selected CAMS sites. The selected sites had different land use classifications (identified in the table) in USGS and TFS-LULC data. Most of the selected sites showed less temperature biases in the MM5-TFS simulation. The wind speed bias was also reduced in the MM5-TFS simulation.

6. Conclusion

A previous MM5 simulation with the Noah LSM using the default USGS-LULC data over-predicted maximum temperatures for Houston because the entire city was inadequately characterized as an impervious surface type. Although the temperature bias could be reduced with the addition of canopy water, a more fundamental approach is to utilize an accurate LULC dataset that represents detailed land use features of the Houston–Galveston area. The satellite-based TFS-LULC data demonstrated the benefits of using the improved data. MM5 simulations with TFS-LULC data successfully predicted the temperature structures in the Houston downtown city area, eliminating the need to add canopy water.

The simulations showed a direct response of meteorological conditions to the underlying land surface features, in particular, when the large-scale flow was weak. For example, on 27 August 2000 when the strong southerly flow dominated, use of different LULC data showed little effect. But on the 25 and 30 of August 2000, when the synoptic flows were weak, the MM5-TFS showed that the asymmetrically elongated Houston heat island convergence zone increased strength of the sea breeze flow and changed the location of the afternoon Gulf of Mexico seabreeze front compared to the MM5-USGS simulations. When the center of Houston was specified as a contiguous impervious urban surface in the USGS data, the MM5-USGS produced a convergent flow in the Houston downtown area that induced stronger bay breeze flow. The hodograph comparisons at the Clinton and La Porte sites demonstrated that the local circulation was successfully reproducing turning of the offshore into onshore flow in the MM5-TFS simulation.

We also noticed that the Houston Ship Channel area was correctly represented as a water body in the TFS-LULC data, and a shallower PBL height was predicted from the MM5-TFS simulation in the water body cell. Because there are enormous emission sources located in the Ship Channel area, utilization of the TFS-LULC data, which predicted the area to be stable with shallow PBL heights, would greatly impact air quality prediction. The detailed description of the land surface processes, such as vegetation evapotranspiration and moisture diffusion processes included in Noah LSM, was invaluable towards gaining a better understanding of the effect of LULC changes on boundary layer dynamics.

This paper is part I of a two-part study and we demonstrated that the changes of the LULC data significantly modify the surface heat flux conditions as well as the local flow pattern, which are the key parameters determining air quality condition. In part II, effects of using two different MM5 results for air quality modeling are discussed.

Acknowledgments

The research described in this article has been funded in part by the Houston Advanced Research Center (HARC) H17: Modeling Effects of Land Use/Land Cover Modifications on the Urban Heat Island Phenomena in Houston, Texas, Grant 077UHH2072A from the Texas Air Research Center (TARC), and the United States Environmental Protection Agency through Grant Agreement Number: EM-83330601-0 to the University of Houston. However, it has not been subjected to the Agency's required peer and policy review and therefore does not necessarily reflect the views of the Agency and no official endorsement should be inferred. Thanks are extended to Dr. Soontae Kim for processing the TFS-LULC data for the MM5 simulations and to Dr. Nielsen-Gammon for the assistance of the meteorological simulation setup.

References

ATMET, 2003. MM5 simulations for TexAQS 2000 episode. Final Report to Houston Advanced Research Center/Texas Environmental Research Consortium (TERC), 101 pp.

Banta, R.M., Senff, C.J., Nielsen-Gammon, J.W., Darby, L.S., Ryerson, T.B., Alvarez, R.J., Sandberg, S.P., Williams, E.J., Trainer, M., 2005. A bad air day in Houston. Bulletin of the American Meteorological Society 86 (5), 657–669, doi:10.1175/BAMS-86-5-657.

Burian, S.J., Stenson, S., Han, W., Ching, J., Byun, D.W., 2004. High-resolution dataset of urban canopy parameters for Houston, Texas. In: Extended Abstract, Fifth Conference on Urban Environment, Vancouver, BC. American Meteorological Society.

Byun, D.W., Kim, S.T., Czader, B., Cheng, F.Y., Stetson, S., Nowak, D., Bornstein, R., Estes, M., 2005. Modeling effects of land use/land cover modifications on the urban heat island phenomenon and air quality in Houston, Texas, Supplemental. HARC Project H17A Supplemental Final Report.

Chen, F., Dudhia, J., 2001. Coupling an advanced land surface-hydrology model with the Penn State-NCAR MM5 modeling system. Part I: model implementation and sensitivity. Monthly Weather Review 129, 569–585.

Chen, F., 2005. Developing an integrated urban modeling system for WRF. In: NCEP EMC Seminar, Camp Springs, 18 October, 2005.

Cheng, F.Y., Byun, D.W., Kim, S.B., 2003. Sensitivity study of the effects of land surface characteristics on meteorological simulations during the TexAQS 2000 period in the Houston–Galveston area. In: Extended

Abstract, 13-th Penn State/NCAR MM5 User's Workshop, Boulder, CO. National Center for Atmospheric Research.

Cheng, F.Y., Byun, D.W., Kim, S.T., 2004. Fine scale meteorological simulations of the Houston–Galveston metropolitan area with LANDSAT-derived high-resolution land use and land cover datasets. In: Extended Abstract, Fifth Conference on Urban Environment, 23–26 August, Vancouver, Canada, 2004.

Cheng, F.-Y., Kim, S.T., Byun, D.W., 2008. Application of high resolution land use and land cover data for atmospheric modeling in the Houston–Galveston metropolitan area: part II, air quality simulation results. Atmospheric Environment 42 (20), 4853–4869.

Civerolo, K.L., Hogrefe, C., Ku, J.Y., Solecki, W., Small, C., Oliveri, C., Cox, J., Kinney, P., 2005. Simulating the effects of urban-scale land use change on surface meteorology and ozone concentrations in the New York City metropolitan region. In: Extended Abstract, Seventh Conference on Atmospheric Chemistry, San Diego, CA. American Meteorological Society.

Grell, G., Dudhia, J., Stauffer, D.R., 1994. A description of the fifth-generation Penn State/NCAR Mesoscale Model (MM5). NCAR Tech. Note NCAR/TN-398 + STR, 117 pp.

GEM, 2003. Satellite data processing for land use and cover type classification. Final Report, TFS-3-027, Prepared for the Texas Forest Service.

Hong, S.Y., Pan, H.L., 1996. Nonlocal boundary layer vertical diffusion in a medium-range forecast model. Monthly Weather Review 124, 2322–2339.

Lam, J.S.L., Lau, A.K.H., Fung, J.C.H., 2006. Application of refined land-use categories for high resolution mesoscale atmospheric modeling. Boundary Layer Meteorology 119, 263–288.

Liu, Y., Chen, F., Warner, T., Swerdlin, S., Bowers, J., Halvorson, S., 2004. Improvements to surface flux computations in a non-local-mixing PBL scheme, and refinements to urban processes in the NOAH land-surface model with the NCAR/ATEC Real-Time FDDA and forecast system. In: 20th Conference on Weather Analysis and Foreascting/16th Conference on Numerical Weather Prediction, 11–15 January 2004, Seattle, Washington.

Lo, C.P., Quattrochi, D.A., 2003. Land use and land cover change, urban heat island phenomenon, and health implications: a remote sensing approach. Photogrammetric Engineering and Remote Sensing 69, 1053–1063.

Nielsen-Gammon, J.W., 2001. Initial modeling of August 2000 Houston–Galveston ozone episode. Report to the Technical Analysis Division, Texas Natural Resource Conservation Commission, December 2001, 71 pp.

Nielsen-Gammon, J.W., 2002a. Evaluation and comparison of preliminary meteorological modeling for the August 2000 Houston–Galveston ozone episode. Report to the Technical Analysis Division, Texas Natural Resource Conservation Commission, February 5, 2002, 83 pp.

Nielsen-Gammon, J.W., 2002b. Meteorological modeling for the August 2000 Houston–Galveston ozone episode: PBL characteristics, nudging procedure and performance evaluation. Report to the Technical Analysis Division, Texas Natural Resource Conservation Commission, February 28, 2002, 109 pp.

Noilhan, J., Planton, S., 1989. A simple parameterization of land surface processes for meteorological models. Monthly Weather Review 117, 536–549.

Senff, C., Banta, R., Darby, L.S., Angevine, W., White, A., Berkowitz, C., Doran, C., 2002. Spatial and temporal variations in mixing heights in Houston. Final Report for TNRCC Project F-20.

Stetson, S.W., 2004. Surface Roughness and Z_0 Parameter Measured from Satellite-based Synthetic Aperture Radar. Research Report. Global Environment Management, Inc.